

Nitrogen Doped Graphene Quantum Dots as Possible Substrates to Stabilize Planar Conformer of Au₂₀ Over its Tetrahedral Conformer: A Systematic DFT Study.

Sharma SRKC Yamijala¹, Arkamita Bandyopadhyay², and Swapan K Pati ^{*2,3,*}

¹Chemistry and Physics of Materials Unit, Jawaharlal Nehru Centre for Advanced Scientific Research, Bangalore 560064, India.

²New Chemistry Unit, Jawaharlal Nehru Centre for Advanced Scientific Research, Bangalore 560064, India.

³Theoretical Sciences Unit, Jawaharlal Nehru Centre for Advanced Scientific Research, Bangalore 560064, India.

*Corresponding author

Abstract

Utilizing the strengths of nitrogen doped graphene quantum dot (N-GQD) as a substrate, here in, we have shown that one can stabilize the catalytically more active planar Au₂₀ (P-Au₂₀) compared to the thermodynamically more stable tetrahedral structure (T-Au₂₀) on an N-GQD. Clearly, this simple route avoids the usage of traditional transition metal oxide substrates which have been suggested and used for stabilizing the planar structure for a long time. Considering the experimental success in the synthesis of N-GQDs and in the stabilization of Au nanoparticles on N-doped graphene, we expect our proposed method to stabilize planar structure will be realized experimentally and will be useful for industrial level applications.

Keywords: Dimensionality crossover, Ab-initio calculations, Bi-layer graphene, Charge transfer, Catalysis.

1 Introduction

Stability, ionization potential, electronic, magnetic, optical and catalytic properties of gold clusters depend not only on their size but also on their shape and charge state.^{1–4} Stabilizing a particular conformer among the others, to achieve the desired properties, is one of the active fields of research.^{3,5–13} When gold clusters are grown on a substrate, the nature of the substrate highly dictates the stability of the conformer, and hence, also its shape. In the past years, a

*pati@jncasr.ac.in

large number of studies have been carried out on several substrates mainly to understand the substrate properties in stabilizing a particular conformer of the gold cluster. Many of these studies have concentrated on stabilizing the catalytically active planar conformer of Au_{20} cluster (P- Au_{20}) over the thermodynamically stable tetrahedral conformer (T- Au_{20})^{3,5-12} and these studies have used metal oxides substrates, such as, MgO ,^{5-8,10,12} CaO ^{3,11,12} etc.

In gas phase, tetrahedral conformer is found to be the most stable conformer both by experimental^{14,15} and by several theoretical studies.^{2,9} Same trend in the stability has been found even when Au_{20} is on pristine MgO , CaO substrates.^{3,5-12} Apart from its thermodynamic stability, T- Au_{20} also has a larger HOMO-LUMO gap (1.77 eV) compared to its other two-dimensional conformers.^{2,9} Thus, it is chemically more stable (or less reactive), and hence, not very useful for catalytic applications. Less reactivity of T- Au_{20} compared to P- Au_{20} has already been proved during the catalytic conversion of CO to CO_2 in the presence of O_2 on a Mo-doped MgO substrate.⁷ Also, theoretical calculations have shown that both the electron accepting and donating capabilities of P- Au_{20} are more compared to that of T- Au_{20} and such trend has been found to be common for planar clusters.⁹ Thus, to utilize the gold clusters in catalytic applications, it is required to stabilize “less stable but catalytically more active” conformers than the “less reactive and thermodynamically more stable” conformers.

Several previous works have shown different ways to stabilize the planar conformer of Au_{20} .^{3,5-12} Most of these works considered metal-oxides as substrates and the methods used to tune the morphology of Au_{20} include (i) depositing thin metal-oxide films on transition metals^{3,5-7} (ii) application of external field⁸ when depositing bulk metal-oxides on transition metals and (iii) to add external dopants^{3,10-12} to bulk metal-oxides without depositing them on transition metals etc. Unlike earlier works, in this study we have considered graphene quantum dots (GQDs),¹⁶⁻¹⁹ the zero-dimensional analogues of graphene, as substrate. We have considered different possibilities like external doping by substituting the carbon atoms of GQD with nitrogen or boron atoms, increasing the doping concentration, introduction of defects, increasing the number of layers of GQDs etc. to see whether we can stabilize P- Au_{20} over T- Au_{20} on GQDs. The main reason behind the consideration of GQDs as substrate is mainly due to a recent report by Li et. al. on the successful preparation and stabilization of Pd nanoparticles (NPs) on top of colloidal GQDs,²⁰ where their main focus was on the Pd-carbon interaction. The same group (and also several other groups) has also shown the successful synthesis of N-doped GQDs (NGQDs) with precise control over the position of the dopant nitrogen.^{21,22} Though, both experimental and theoretical works exist on the interaction of Au clusters with N-doped graphene (not GQDs), they didn’t concentrate on tuning the morphology of Au clusters. In this work, we have shown that, nitrogen doped GQDs can act as alternative substrates to doped metal-oxide substrates in stabilizing the P- Au_{20} over T- Au_{20} .

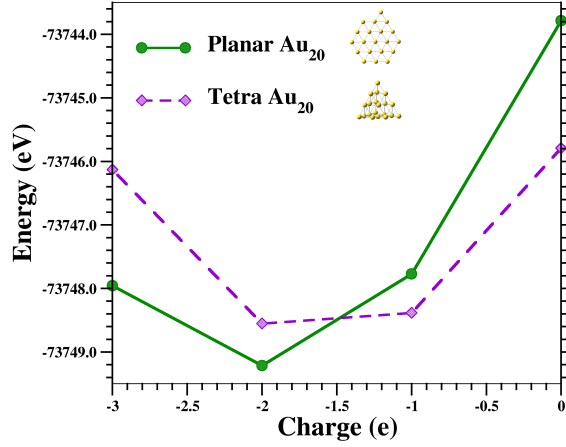


Figure 1: Energy of P-Au₂₀ vs T-Au₂₀ as a function of charge. Observe the dimensionality cross-over at a charge of -2.

2 Results and Discussions

In previous works,^{5,6,8-11} it has been clearly mentioned that the main reason for the stability of P-Au₂₀ over T-Au₂₀ on a doped metal-oxide substrate is due to the greater charge transfer from the substrate to P-Au₂₀ than to T-Au₂₀ (and also due to the greater charge accumulation at the cluster-substrate interface). But, these works didn't explain why there is a requirement of an oxide substrate if charge transfer is the sole reason for the stability of P-Au₂₀. To address this issue, first we have performed a series of calculations (at B3LYP/LANL2DZ level of theory) on both P and T-Au₂₀ clusters with different charges (in gas phase) and we find that the planar structure can be stabilized over tetrahedral structure when charge on the system is -2 or more, as shown in figure 1 (see Supporting Information (SI) to know the functional/basis-set dependency). Apart from this, in a previous work,¹⁰ it has been shown that P-Au₂₀ can be stabilized over T-Au₂₀ on an Al-doped MgO substrate when substrate transfers ~ 0.9 e or more to the clusters. Thus, these results suggest that, even though a substrate is not necessary to stabilize P-Au₂₀ over T-Au₂₀, it will help to reduce the required amount of charge transfer in stabilizing P-Au₂₀. To further prove the non-necessity of an oxide-substrate in stabilizing the planar conformer, we have considered a single layer graphene quantum dot (GQD) as our substrate and further calculations have been performed (at BLYP+DFT-D3/DZP level of theory).

In Table 1, we have given the energy difference ($E_{diff} = E_T - E_P$) between the T-Au₂₀ and P-Au₂₀ clusters when they are isolated (i. e. not on any substrate) and when they are on different substrates. Firstly, in accordance with several previous studies, we find that the tetra conformer is more stable (negative value of $E_T - E_P$) than the planar conformer when the clusters are isolated. We find the same trend even when the clusters are on a GQD substrate, although the energy difference (E_{diff}) has reduced drastically (by ~ 3 eV). In fact, we find that this reduced E_{diff} is due to the larger substrate-cluster interaction (SCI) for the case of P-Au₂₀ than for T-Au₂₀, which in turn is due to the shape

Table 1: Energy difference between P-Au₂₀ and T-Au₂₀ when they are isolated and when they are on different substrates along with the energy of substrate cluster interaction (E_{SCI}) is given for all the systems.

Systems	Energy (eV)	$E_T - E_P$ (eV)	E_{SCI} (eV)
P-Au ₂₀	-17992.686		
T-Au ₂₀	-17996.651	-3.965	
GQD	-35840.945		
P-Au ₂₀ @GQD	-53840.212		-6.582
T-Au ₂₀ @GQD	-53841.025	-0.813	-3.429
N-GQD	-35955.676		
P-Au ₂₀ @N-GQD	-53955.573		-7.211
T-Au ₂₀ @N-GQD	-53955.853	-0.280	-3.526
2N-GQD	-36070.362		
P-Au ₂₀ @2N-GQD	-54070.726		-7.679
T-Au ₂₀ @2N-GQD	-54070.701	0.025	-3.688
3N-GQD	-36185.150		
P-Au ₂₀ @3N-GQD	-54185.571		-7.736
T-Au ₂₀ @3N-GQD	-54185.454	0.117	-3.653
4N-GQD	-36299.796		
P-Au ₂₀ @4N-GQD	-54300.703		-8.222
T-Au ₂₀ @4N-GQD	-54300.194	0.509	-3.747
5N-GQD	-36414.411		
P-Au ₂₀ @5N-GQD	-54415.489		-8.392
T-Au ₂₀ @5N-GQD	-54414.844	0.645	-3.782
6N-GQD	-36529.330		
P-Au ₂₀ @6N-GQD	-54530.402		-8.386
T-Au ₂₀ @6N-GQD	-54529.753	0.649	-3.773
B-GQD	-35762.547		
P-Au ₂₀ @B-GQD	-53761.879		-6.646
T-Au ₂₀ @B-GQD	-53762.818	-0.939	-3.620
pyN-GQD	-36030.984		
P-Au ₂₀ @pyN-GQD	-54030.291		-6.621
T-Au ₂₀ @pyN-GQD	-54031.167	-0.876	-3.532

of the P-Au₂₀ which allows all of its atoms to interact with the substrate. We have quantified the energy of SCI (E_{SCI}) as below: $E_{SCI} = E_{tot} - E_{sub} - E_{Au}$, where, E_{tot} is the total energy of the cluster on a substrate; E_{sub} and E_{Au} are the energies of the isolated substrate and the Au cluster, respectively, and the values are given in table 1. Clearly, E_{SCI} for P-Au₂₀ is ~ 3 eV greater than the T-Au₂₀, when these clusters are on a GQD substrate. Also, we find that (see table S1 of SI) there is ~ 1 e charge transfer (CT) to P-Au₂₀ from GQD, where as, it is only ~ 0.2 e for T-Au₂₀. Thus, we find that, though P-Au₂₀ has acquired higher amount of charge from GQD substrate and has larger E_{SCI} (when compared with T-Au₂₀), its stability is still less than that of T-Au₂₀. This higher stability of T-Au₂₀ on a GQD substrate is some what similar to what previously has been observed for the cases of MgO and CaO substrates^{5,6,8-11} suggesting that our choice of substrate is correct and further necessary steps have to be taken in order to acquire the required stability of P-Au₂₀. Among the several previously implemented techniques, we find doping the substrate with electron rich species¹⁰⁻¹² as one of the simple and successful technique for stabilizing P-Au₂₀ over T-Au₂₀ and we have doped our GQD substrates with nitrogen (N) atoms.

Doping GQDs with N atoms can be of several ways, for example, pyridinic, pyrrolic, substitutional [replacing C with N] etc. Experimental studies on gold clusters stabilized on N-doped graphene have shown that²² (i) substitutional and pyrrolic (pyridinic) doping leads to n-type (p-type) graphene and (ii) dopant nitrogen sites in an n-type graphene serves as electron donors and gold clusters acts as electron acceptors. To verify these results, we have optimized the gold clusters on both substitutionally doped N-GQD and pyridinic N-GQD (pyN-GQD). In agreement with these results, we find a decrease (increase) in the negative “ $E_T - E_P$ ” value, compared to that of pristine GQD, when doping is substitutional (pyridinic). As our main aim is to stabilize P-Au₂₀, i.e. to attain a positive “ $E_T - E_P$ ” value, we have performed all our further calculations only with substitutional doping. We have varied the doping concentration from 0.44 % (i. e. one N atom in 228 C atoms) to 2.63 % (6 N atoms in 228 C atoms) and while doping more than one nitrogen, we have considered the experimental results of N-doped graphene²³ and doped only the carbon atoms belonging to same sub-lattice.

In Table 1, we have given “ $E_T - E_P$ ” values for all the different concentrations considered. Clearly, the most stable conformer of Au₂₀ on a GQD substrate has changed from tetra to planar for all the nitrogen dopant concentrations greater than ~ 0.88 % (for the present level of theory) and we find an increase in the stability of P-Au₂₀ with the increase in the dopant concentrations. This is an interesting result, because it proves the non-necessity of an oxide substrate for stabilizing catalytically active P-Au₂₀ conformer. Many N-doped GQDs and graphene sheets have been synthesized.²⁰⁻²³ So, we checked the robustness of our result against (i) the dopant atoms position (ii) number of GQD layers (iii) exchange-correlation functional. Firstly, for 2.63 % concentration, we find that P-Au₂₀ is, at least, ~ 0.26 eV more stable than T-Au₂₀, even when all the dopant atoms are in a single zigzag line of a GQD (which is not a favorable way of doping²³). Next, as the experimentally produced GQDs generally contain more than one layer, we have also considered bi-layered GQDs. With an increase in the number of layers, we find that the stability of P-Au₂₀ has further increased for the same number of dopant N-atoms. For example, when substituting with

two nitrogen atoms stability of P-Au₂₀ has increased from ~ 0.026 eV to ~ 0.1 eV when moved from monolayer GQD to bi-layer GQD. Similarly, when substituted with six nitrogen atoms, the stability has raised by ~ 0.3 eV for bi-layer GQD. Finally, we have changed the exchange correlation functional and found that the trend is still maintained, although the amount of gain in the stability is less (see SI). Thus, based on our results and on the available experimental methods for growing N-GQDs as well as gold clusters on N-doped graphene, we conjecture that experimentalists would find a dimensionality cross-over from T-Au₂₀ to P-Au₂₀ on N-GQDs.

Finally, to know the possible catalytically active sites of Au₂₀ clusters, when supported on a N-GQD, we have plotted the iso-surfaces of charge transfer between N-GQD and Au₂₀ clusters as shown in figure 2. To plot the iso-surfaces of charge transfer, total electron density of the composite system (i.e. N-GQD + Au₂₀) has been subtracted from the total electron density of the substrate and the cluster with the same geometry (i.e. without any further optimization). From these plots, it is clear that, major changes in the charge of the substrate occurred only for the atoms which are below the Au₂₀ clusters. In the case of clusters, major changes have occurred for the corner atoms than for the atoms which are in the middle. Among T-Au₂₀ and P-Au₂₀ clusters, P-Au₂₀ has large number of corner atoms and more number of atoms directly interacting with the substrate. Also, we notice that the amount of charge accumulated at the substrate cluster interface is more for P-Au₂₀ than for T-Au₂₀. Finally, for T-Au₂₀, only those atoms which are directly above the N-GQD substrate have acquired more negative charge compared to the ones in the upper layers. Thus, based on all these results and earlier reports^{5,8,10} we expect that corner atoms of both the clusters will act as active sites for catalytic applications and between P-Au₂₀ and T-Au₂₀, the former with more active sites should be catalytically more active than T-Au₂₀.

3 Conclusions

In conclusion, motivated by the recent successful synthesis of colloidal GQDs and N-GQDs with precise control over the number of atoms, position of the dopants and their application in stabilizing Pd nanoparticles, we have investigated several possibilities of utilizing these doped/un-doped GQDs to stabilize the catalytically more useful P-Au₂₀ compared to the thermodynamically more stable T-Au₂₀. Both single-layer and bi-layer GQDs, with and without nitrogen dopants, have been considered and we find that binding energy of P-Au₂₀ towards GQD is more (~ 3 eV) compared to T-Au₂₀ and it is much more when the GQDs are doped with nitrogen and is even more when the GQDs are bi-layered. Different concentrations of nitrogen doping have been considered and we find that, P-Au₂₀ can be stabilized over T-Au₂₀, thermodynamically, by ~ 1 eV when the N-dopant concentration is ~ 1.3 % (i.e. 1N-atom for every 76-C atoms) in bi-layer GQDs. Also, from charge transfer plots, we find that P-Au₂₀ has more active sites for catalysis. The main point is that stronger interaction of P-Au₂₀ with N-GQD compared to T-Au₂₀ is due to its large contact area with N-GQD substrate and also its ability to accept more electrons.

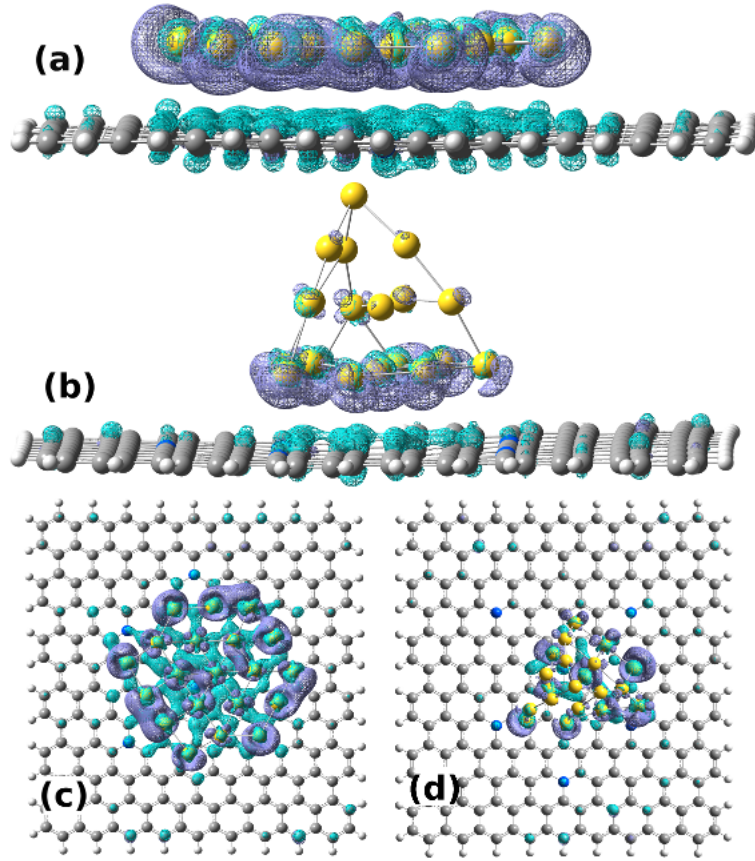


Figure 2: Isosurface contours depicting the charge transfer process from substrate to Au_{20} clusters. Top, bottom views of P- Au_{20} are shown in (a), (c) and of T- Au_{20} in (b), (d). Iso-value of $0.001 \text{ e}/\text{\AA}^3$ is used for all the plots. Cyan color depicts loss in electron density.

4 Computational Details

Previous studies on the interaction between graphene and transition metal clusters suggests that dispersion forces are important to exactly mimic the interaction between gold and graphene and these studies have also shown that the empirical dispersion correction i. e. DFT-D3 is sufficient to reproduce the results obtained with the best methods (EE+vdW for Au-graphene; EE+vdW, M06-2X and MP2 calculate data in latexlations for Au-coronene interactions) described in these works for graphene and gold interaction.²⁴ We have performed all the calculations using spin-unrestricted density functional theory with Becke-Lee-Yang-Parr (BLYP) GGA exchange-correlation functional,^{25,26} along with Grimme’s DFT-D3 dispersion correction,²⁷ as implemented in the QUICKSTEP module of the CP2K package²⁸ (unless otherwise mentioned explicitly). We have used the norm-conserving Goedecker–Teter–Hutter (GTH) pseudopotentials,^{29–31} which are optimized in CP2K package to use them along with the BLYP functional. CP2K uses a hybrid Gaussian and plane wave method for the electronic representation.³² In this work, Kohn-Sham valence orbitals have been expanded using double zeta valence polarized basis sets which are optimized for the GTH pseudopotentials (DZVP-MOLOPT-SR-GTH). Together with the NN50 smoothing method, a 320 Ry density cut-off is used for the auxiliary basis set of plane waves. To avoid any unwanted interaction with the periodic images, we have considered a $38 \times 38 \times 38$ Å cubic unit cell along with the poisson^{33,34} solver (to ensure the non existence of wave function after the edges of the simulation box). Geometry optimizations have been performed using BFGS method and systems are optimized till the force on each atom is less than 0.0001 Hartree/Bohr. G09 package³⁵ has been used to perform all the calculations on isolated gold clusters using different exchange-correlation functionals, namely, PBE, BLYP, B3LYP and M06-2X with LANL2DZ basis set and LANL2 pseudopotentials.

References

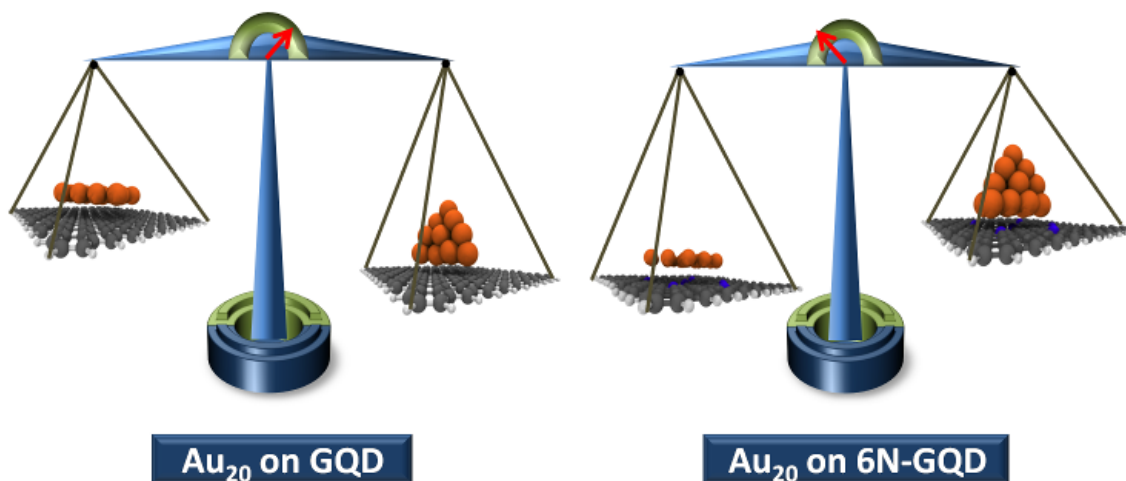
- [1] Jain, P. K. *Angewandte Chemie International Edition* **2014**, *53*, 1197–1197.
- [2] Kryachko, E. S.; Remacle, F. *International Journal of Quantum Chemistry* **2007**, *107*, 2922–2934.
- [3] Shao, X.; Nilius, N.; Freund, H.-J. *Phys. Rev. B* **2012**, *85*, 115444.
- [4] Nijamudheen, A.; Datta, A. Effects of Charging on the Structural and Electronic Properties of Aun Nanoclusters (n = 2-20). Nanoscience, Technology and Societal Implications (NSTSI), 2011 International Conference on. 2011; pp 1–5.
- [5] Ricci, D.; Bongiorno, A.; Pacchioni, G.; Landman, U. *Phys. Rev. Lett.* **2006**, *97*, 036106.
- [6] Sterrer, M.; Risse, T.; Heyde, M.; Rust, H.-P.; Freund, H.-J. *Phys. Rev. Lett.* **2007**, *98*, 206103.
- [7] Zhang, C.; Yoon, B.; Landman, U. *Journal of the American Chemical Society* **2007**, *129*, 2228–2229.

- [8] Yoon, B.; Landman, U. *Phys. Rev. Lett.* **2008**, *100*, 056102.
- [9] Martinez, A. *The Journal of Physical Chemistry C* **2010**, *114*, 21240–21246.
- [10] Mammen, N.; Narasimhan, S.; Gironcoli, S. d. *Journal of the American Chemical Society* **2011**, *133*, 2801–2803.
- [11] Shao, X.; Prada, S.; Giordano, L.; Pacchioni, G.; Nilius, N.; Freund, H.-J. *Angewandte Chemie International Edition* **2011**, *50*, 11525–11527.
- [12] Stavale, F.; Shao, X.; Nilius, N.; Freund, H.-J.; Prada, S.; Giordano, L.; Pacchioni, G. *Journal of the American Chemical Society* **2012**, *134*, 11380–11383.
- [13] Nijamudheen, A.; Jose, D.; Datta, A. *Computational and Theoretical Chemistry* **2011**, *966*, 133 – 136.
- [14] Li, J.; Li, X.; Zhai, H.-J.; Wang, L.-S. *Science* **2003**, *299*, 864–867.
- [15] Gruene, P.; Rayner, D. M.; Redlich, B.; van der Meer, A. F. G.; Lyon, J. T.; Meijer, G.; Fielicke, A. *Science* **2008**, *321*, 674–676.
- [16] Yamijala, S. S.; Bandyopadhyay, A.; Pati, S. K. *The Journal of Physical Chemistry C* **2013**, *117*, 23295–23304.
- [17] Bandyopadhyay, A.; Yamijala, S. S. R. K. C.; Pati, S. K. *Phys. Chem. Chem. Phys.* **2013**, *15*, 13881–13887.
- [18] Yamijala, S. S.; Bandyopadhyay, A.; Pati, S. K. *Chemical Physics Letters* **2014**, *603*, 28 – 32.
- [19] Hod, O.; Barone, V.; Scuseria, G. E. *Phys. Rev. B* **2008**, *77*, 035411.
- [20] Yan, X.; Li, Q.; Li, L.-s. *Journal of the American Chemical Society* **2012**, *134*, 16095–16098.
- [21] Yan, X.; Li, B.; Li, L.-s. *Accounts of Chemical Research* **2013**, *46*, 2254–2262.
- [22] Xie, X.; Long, J.; Xu, J.; Chen, L.; Wang, Y.; Zhang, Z.; Wang, X. *RSC Adv.* **2012**, *2*, 12438–12446.
- [23] Zhao, L. et al. *Science* **2011**, *333*, 999–1003.
- [24] Granatier, J.; Lazar, P.; Otyepka, M.; Hobza, P. *Journal of Chemical Theory and Computation* **2011**, *7*, 3743–3755.
- [25] Becke, A. D. *Phys. Rev. A* **1988**, *38*, 3098–3100.
- [26] Lee, C.; Yang, W.; Parr, R. G. *Phys. Rev. B* **1988**, *37*, 785–789.
- [27] Grimme, S.; Antony, J.; Ehrlich, S.; Krieg, H. *The Journal of Chemical Physics* **2010**, *132*, 15.
- [28] VandeVondele, J.; Krack, M.; Mohamed, F.; Parrinello, M.; Chassaing, T.; Hutter, J. *Computer Physics Communications* **2005**, *167*, 103 – 128.

- [29] Hartwigsen, C.; Goedecker, S.; Hutter, J. *Phys. Rev. B* **1998**, *58*, 3641–3662.
- [30] Goedecker, S.; Teter, M.; Hutter, J. *Phys. Rev. B* **1996**, *54*, 1703–1710.
- [31] Krack, M. *Theoretical Chemistry Accounts* **2005**, *114*, 145–152.
- [32] Lippert, B. G.; Hutter, J.; Parrinello, M. *Molecular Physics* **1997**, *92*, 477–488.
- [33] Genovese, L.; Deutsch, T.; Neelov, A.; Goedecker, S.; Beylkin, G. *The Journal of Chemical Physics* **2006**, *125*, 7.
- [34] Genovese, L.; Deutsch, T.; Goedecker, S. *The Journal of Chemical Physics* **2007**, *127*, 5.
- [35] Frisch, M.; Trucks, G.; Schlegel, H.; Scuseria, G.; Robb, M.; Cheeseman, J.; Scalmani, G.; Barone, V.; Mennucci, B.; Petersson, G.; others, . *Gaussian, Inc., Wallingford, CT* **2010**,

Graphical TOC entry

Dimensionality cross-over with Doping



P-Au₂₀ becomes more stable than that of T-Au₂₀ after doping GQD substrate with nitrogen atoms.

5 Supporting Information

Additional computational details, table containing charges on individual species for all the systems, charge dependency on exchange-correlation functional are given.

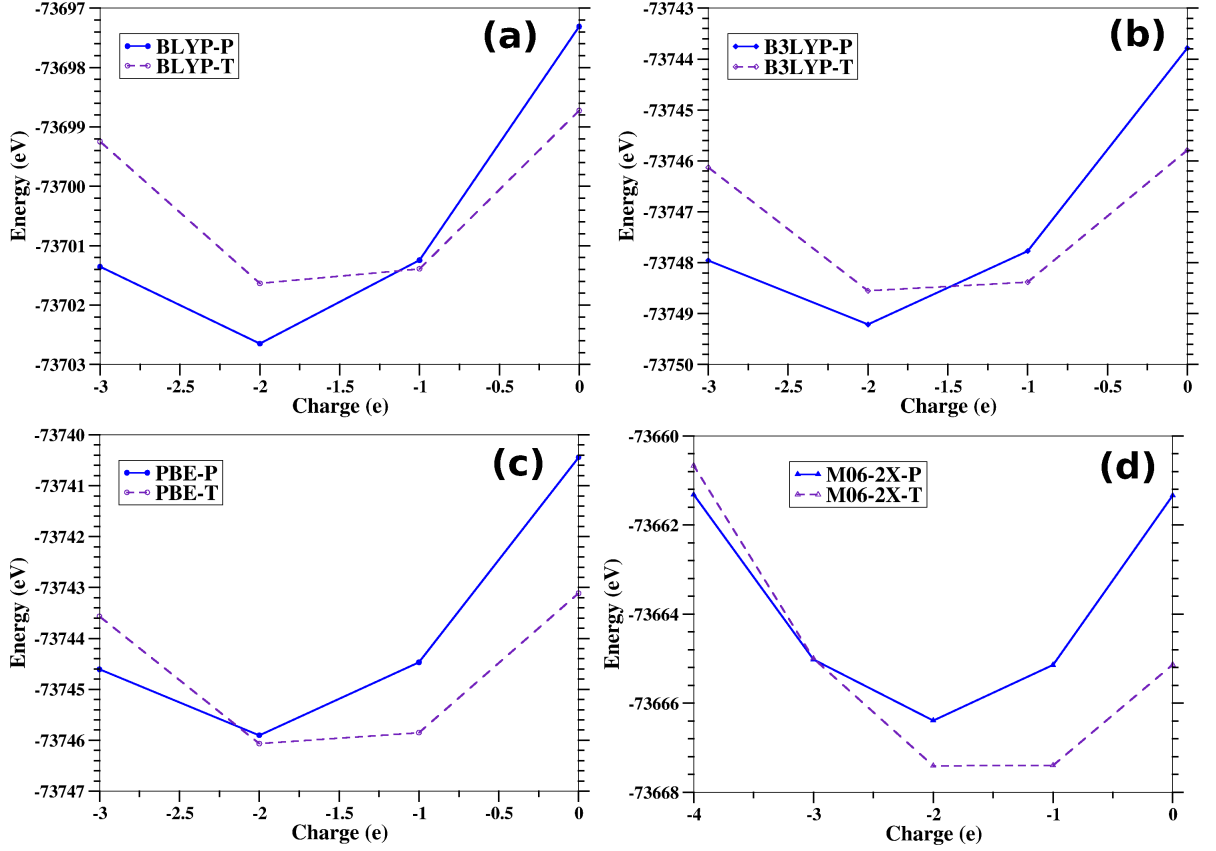


Figure S1: Energy of isolated Au_{20} clusters as a function of charge and exchange-correlation functionals. (a) BLYP (b) B3LYP (c) PBE and (d) M06-2X functionals. P and T in the legends after the functional name denotes planar and tetra conformers, respectively, of Au_{20}

5.1 Charge required to observe a dimensionality crossover as a function of exchange-correlation functional

As shown in Figure S1, the amount of the charge required to obtain the dimensionality crossover depends on the exchange-correlation functional (Exc) used. For BLYP and B3LYP it is between -1 e and -2 e and for PBE and M06-2X it is between -2 and -3 e. Though the amount of charge required varies with Exc, it is clear that, above a particular charge dimensionality crossover will surely occur. Also, as mentioned in the main article, this amount will change when the clusters are kept on a substrate.

5.2 Robustness check for stability of P- Au_{20} over T- Au_{20} on N-doped GQDs with PBE functional

From our calculations using PBE functional (by keeping all the other parameters like cutoff, box length etc. of the BLYP functional), we find that P- Au_{20} is less

stable than T-Au₂₀ on both monolayer and bi-layer GQDs even when six carbon atoms are replaced with nitrogen atoms (though the difference has reduced to as less as ~ 0.1 eV). But, with tri-layer GQDs, we find that P-Au₂₀ has more stability than T-Au₂₀ (by ~ 0.03 eV) when tri-layer GQDs are doped with six nitrogen atoms. Further calculations with higher concentrations are under progress and will be published else where. Thus, our results are robust against change in the Exc and from these results we conjecture that experimentalists would soon realize P-Au₂₀ clusters on N-doped few layer GQDs.

5.3 Additional Computational Details

It is important to mention that, BLYP calculations, in general, took more time to converge compared to PBE calculations. Also, we find that energy fluctuations are huge at the initial stages (some times even for 200 optimization steps) of geometry optimization using BLYP. Though the suggested remedies like decrease in the energy gap or using FULL-SINGLE-INVERSE were helpful for monolayer studies and bi-layer studies (although they also took huge time), they didn't help for tri-layer studies. Though an increase in plane wave cutoff (i. e. more than 320 Ry) may solve the problem, we couldn't use it because of the issues in the memory (RAM) while running the jobs (on our clusters).

6 Acknowledgements

S.S.R.K.C.Y., A.B. and S.K.P. acknowledge TUE-CMS, JNCASR for the computational facilities. S.K.P. acknowledges DST for funding. A.B. acknowledges UGC for JRF.

Table 2: Charges on the individual atoms (Mülliken charges) in the respective systems. Amount of the charge transferred to the gold clusters from the substrates can be directly identified by seeing column 3 (GOLD). Gain/loss of electron charge can be seen by comparing the respective systems with the isolated systems. For example, by comparing P-Au₂₀@GQD with GQD and P-Au₂₀, we can notice that, carbon has lost ~ 0.95 e charge and the same has been gained by gold.

Systems	CARBON	GOLD	NITROGEN	BORON	HYDROGEN
P-Au ₂₀	0.00	0.00	0.00	0.00	0.00
T-Au ₂₀	0.00	0.00	0.00	0.00	0.00
GQD	-1.75	0.00	0.00	0.00	1.75
P-Au ₂₀ @GQD	-0.83	-0.95	0.00	0.00	1.79
T-Au ₂₀ @GQD	-1.58	-0.18	0.00	0.00	1.76
N-GQD	-1.71	0.00	-0.03	0.00	1.74
P-Au ₂₀ @N-GQD	-0.75	-1.07	0.04	0.00	1.78
T-Au ₂₀ @N-GQD	-1.59	-0.20	0.04	0.00	1.75
2N-GQD	-1.69	0.00	-0.05	0.00	1.73
P-Au ₂₀ @2N-GQD	-0.42	-1.43	0.07	0.00	1.79
T-Au ₂₀ @2N-GQD	-1.45	-0.34	0.04	0.00	1.75
3N-GQD	-1.65	0.00	-0.08	0.00	1.73
P-Au ₂₀ @3N-GQD	-0.27	-1.62	0.10	0.00	1.79
T-Au ₂₀ @3N-GQD	-1.01	-0.79	0.05	0.00	1.76
4N-GQD	-1.62	0.00	-0.11	0.00	1.72
P-Au ₂₀ @4N-GQD	-0.29	-1.63	0.15	0.00	1.78
T-Au ₂₀ @4N-GQD	-0.99	-0.83	0.07	0.00	1.75
5N-GQD	-1.58	0.00	-0.13	0.00	1.71
P-Au ₂₀ @5N-GQD	-0.25	-1.66	0.15	0.00	1.77
T-Au ₂₀ @5N-GQD	-0.93	-0.87	0.05	0.00	1.75
6N-GQD	-1.53	0.00	-0.18	0.00	1.71
P-Au ₂₀ @6N-GQD	-0.20	-1.71	0.15	0.00	1.76
T-Au ₂₀ @6N-GQD	-0.90	-0.86	0.02	0.00	1.74
B-GQD	-1.63	0.00	0.00	-0.14	1.76
P-Au ₂₀ @B-GQD	-0.77	-0.98	0.00	-0.05	1.80
T-Au ₂₀ @B-GQD	-1.41	-0.35	0.00	-0.02	1.78
pyN-GQD	-1.27	0.00	-0.49	0.00	1.76
P-Au ₂₀ @pyN-GQD	-0.50	-1.02	-0.29	0.00	1.80
T-Au ₂₀ @pyN-GQD	-1.07	-0.42	-0.28	0.00	1.77